On the impact of viscous droplets on wet solid surfaces for spray painting processes

B. Shen*[1], Q. Ye[2], O. Tiedje[2], J. Domnick[1]
[1]University of Applied Sciences Esslingen, Esslingen, Germany
[2]Fraunhofer Institute for Manufacturing Engineering and Automation, Stuttgart, Germany
*Corresponding author email: bo.shen@hs-esslingen.de

Abstract
The present contribution deals with numerical studies of the impact of viscous droplets on solid surfaces, focusing especially on prewetted substrates covered with a thin liquid film during spray painting processes. Numerical simulations using the volume of fluid (VOF) approach were carried out to investigate the evolution of the shape of the impacting droplet. Both Newtonian and non-Newtonian viscous fluids were considered. The evolution of the droplet contour, especially the crater shape and size were estimated in the simulations. Effects of impact conditions and liquid properties on the crater shape and size were analyzed in detail through an appropriate parameter study.

Keywords
Drop impact, liquid film, Cross model, cratering, coalescence

Introduction

The collision of liquid drops with solid surfaces occurs in many engineering applications such as spray painting, spray cooling, and ink-jet printing. This paper presents actual results of a part of a project study of spray painting using viscous paint liquids. The motivation for the investigation lies in the huge industrial demand of understanding air entrapment during drop impact, which may lead to so-called pinholes after drying and baking, and the final wavy surface structure (also called orange peel) in spray painting applications.

The impact of liquid droplets on dry and wet surfaces is a complex multi-phase flow problem and has been of research interest for more than a century [1,2]. The phenomena of drop impact on a wet surface can be classified as floating, bouncing, coalescence and splashing [3]. Many experiments and numerical simulations [4–7] were performed for estimating the thresholds of these phenomena, understanding vortex rings after coalescing impact, determining splashing characteristics and studying entrainment of gas bubbles.

Most of the previous studies were focusing on the splashing impact. These investigations mainly consider low viscous liquids such as water and ethanol. However, liquids used in spray painting processes are fluids with high viscosities and low surface tensions. Their viscosities can be 1 – 3 orders of magnitude greater than the viscosity of water. On the other hand, impact velocities are not as high as, e.g., in steam turbines. Thereby, droplet impacts in spray painting lead mainly to coalescence.

In the present work, the coalescing impact in spray painting was numerically investigated in detail through a parameter study. The non-Newtonian behaviour of paint liquids was also considered in the simulation and represented using the Cross model.

Material and methods

Model paints

Three model paints consisting of varying mass fractions of a basic paint formulation and n-butyl acetate were used in the present study. The shear viscosity was experimentally measured by using a rotational rheometer in the low shear rate range up to 3000 s^{-1} and a capillary rheometer in the high shear rate range up to 10^6 s^{-1}. The measured viscosities as a function of the shear rate are illustrated in Figure 1. Like most of the paint liquids used in industrial applications, the model paints show a non-Newtonian behaviour, namely a shear-thinning behaviour, i.e., the viscosity decreases with increasing shear rate.

This kind of non-Newtonian behaviour was also applied in the simulation. The correlation between viscosity and shear rate is described by using the Cross model, which is also plotted in Figure 1.

$$\eta = \eta_\infty + \frac{\eta_0 - \eta_\infty}{1 + (t \cdot \dot{\gamma})^m}$$

In the above equation η and $\dot{\gamma}$ are the shear viscosity and the shear rate, respectively. η_∞ represents the shear viscosity when the shear rate approaches infinity, η_0 the viscosity when the shear rate approaches zero, the so-called zero viscosity. t and m are consistency index and flow index, respectively.

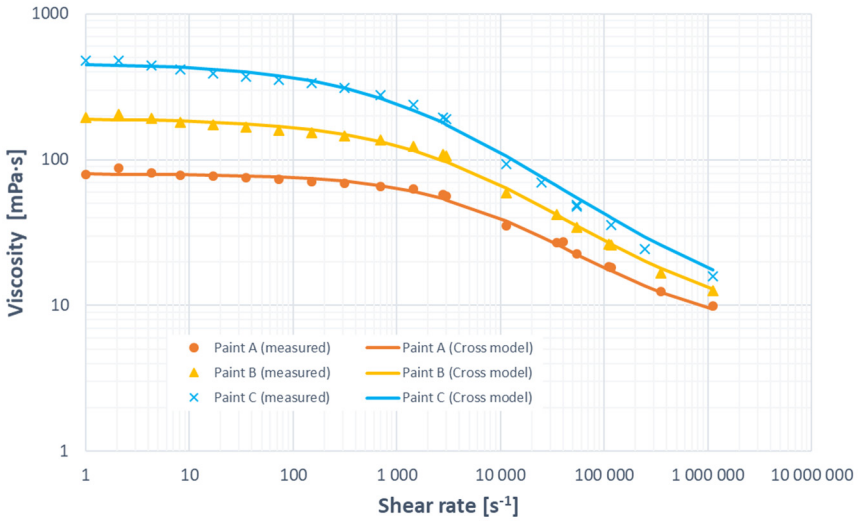

Figure 1. Flow curves of the model paints measured and fitted by the Cross model.

Table 1 – Rheological parameters for the model paints

Model paint	η_0 [mPa·s]	η_∞ [mPa·s]	t [-]	m [-]	ρ [kg/m³]
A	80.05	6.58	1.41e-4	0.63	920.5
B	190.53	7.23	3.66e-4	0.57	928.3
C	455.25	8.13	8.49e-4	0.56	943.3

Table 1 summarizes the rheological parameters for the model paints used in the present study. Each model paint has been applied in two variants with a static surface tension of either 0.024 N/m or 0.067 N/m.

A characteristic viscosity η^* is introduced and defined as the viscosity at the characteristic shear rate $\dot{\gamma}^*$of droplets in the impact process, which is calculated as follows:

$$\dot{\gamma}^* = \frac{2 \cdot u}{d}$$

where u is the impact velocity and d the drop diameter.

Boundary conditions

For describing the droplet size distribution of sprays the volume median Dv50 is frequently used. The Dv50 is defined as the size of the droplet diameter that splits the volume distribution of the spray with half above and half below this size. In spray painting processes, typical values of Dv50 range between 30 and 50 µm are measured. Therefore, droplets with the diameter of 30, 45, 65 and 80 µm were investigated in the present study, taking into account that for some properties the bigger droplets are very relevant. The chosen film thicknesses used in the simulations were 30, 45 and 65 µm, resulting in a ratio between the film thickness and the droplet diameter in a range of 0.375 – 2.167.

Considering the correlation between droplet impact velocity and droplet diameter using different atomizers in spray painting processes shown in Figure 2 [8], impact velocities up to 10 m/s were used in the simulation. Since most of the paint droplets impact close to the normal angle on the surface, oblique impact was not considered in the present investigations so far.

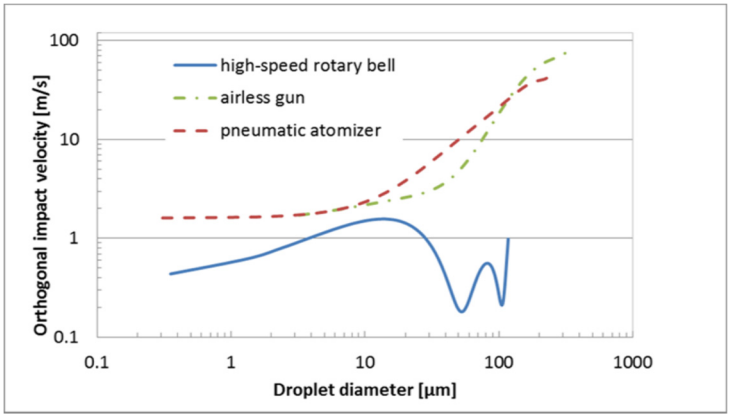

Figure 2. Correlation between droplet impact velocity and droplet diameter using different atomizers in spray painting processes [8].

Characteristic Reynolds and Ohnesorge numbers can be calculated based on droplet properties

$$Re^* = \frac{\rho u d}{\eta^*}$$

$$Oh^* = \frac{\eta^*}{\sqrt{\rho \sigma d}}$$

where ρ and σ are the droplet density and surface tension, respectively, η^* the characteristic viscosity of the droplet, i.e., the viscosity at the characteristic shear rate γ*.

Computational method

The numerical simulations were carried out using the commercial CFD code ANSYS Fluent based on the finite-volume approach. The code was used to solve the unsteady, incompressible, laminar flow in 2D axisymmetric coordinates. The VOF model was used to calculate the two-phase field and to track the gas-liquid interface.

A computational domain of 2000 × 600 µm was used in the simulations. Thus, the ratio between the width of the liquid film, which is patched in the simulation, and the droplet diameter must be greater than 25. The simulative cases can therefore be considered as a droplet impact on an infinite wet solid surface. The basic size of the grid is 8 µm. The grids in the impact region and under the film were refined to 0.25 µm. The overall mesh cell count was approx. 3.5 million.

Results and discussion

Phenomena of droplet impact

As mentioned above, the collision of a droplet with a prewetted solid surface in spray painting processes results usually in coalescence due to the high viscosity of painting materials. When a small droplet with a low impact speed falls onto a wet surface, the target surface is hardly disturbed and a lump is formed above the liquid layer (see Figure 3a). The liquid of the droplet deposits subsequently in the liquid layer. With increasing impact energy of the droplet, namely either with a larger diameter or with a higher velocity, a small crater can be formed in the target liquid layer (see Figure 3b). If the impact energy is high enough, at the circumference of the crater the so-called crater rim rises above the original surface of the target liquid layer (see Figure 3c).

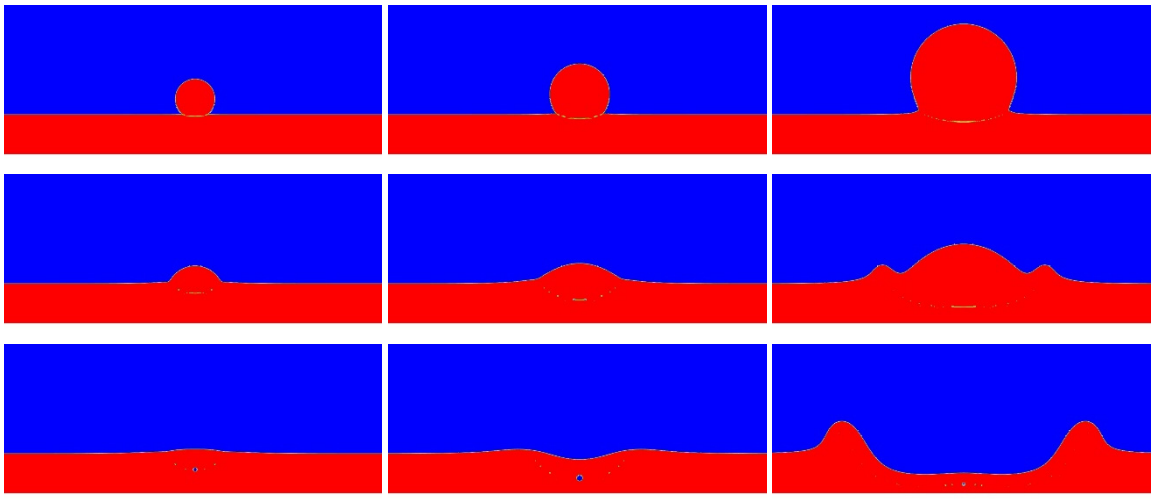

a) b) c)

Figure 3. Phenomena of drop impact on a wet solid surface (red: liquid, blue: air).

In Figure 4, the obtained droplet impact formations are shown in a Reynolds/Ohnesorge plane. Depositing impacts are plotted with blue points and cratering cases with orange circles. A boundary between deposition and cratering can be observed. In general, the impact on a wet surface of a droplet whose Reynolds number is greater than 10 results in a cratering collision. At a low Reynolds number, a crater can also be formed if

$$Oh > 1.43 - 0.091 \cdot Re$$

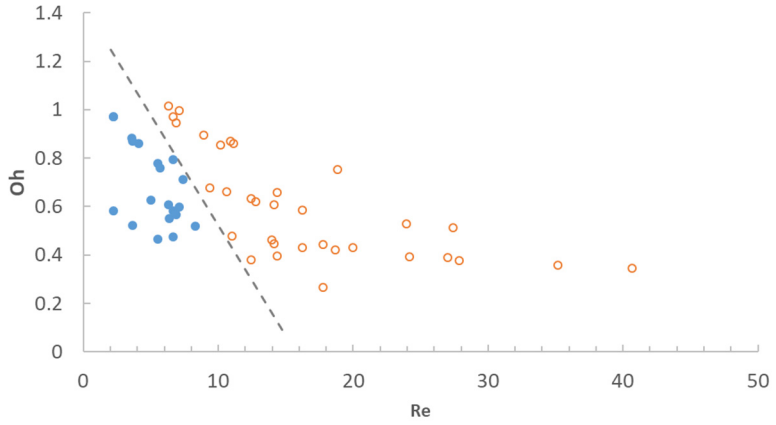

Figure 4. Droplet impact formations at different Reynolds and Ohnesorge numbers.

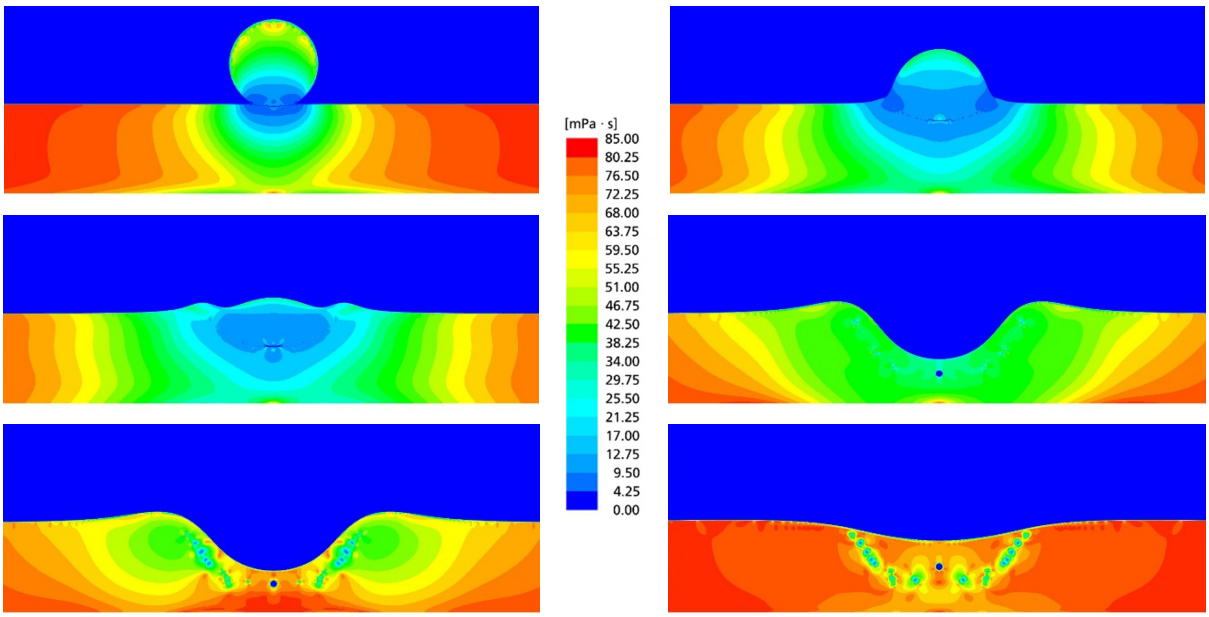

Figure 5. Evolution of the viscosity contours.

Shear thinning in liquids

Figure 5 shows the evolution of the viscosity in the droplet and the liquid film during a cratering process. Here, a droplet of model paint A with the diameter of 65 µm falls with an impact velocity of 6 m/s on a wet solid surface with the a thickness of 65 µm. The characteristic viscosity η^* of the droplet is determined to be 14.86 mPa·s, the Reynold number 24.16 and the Ohnesorge number 0.39. At the early stage of drop impact, the viscosity is quite low in the collision region due to the very high shear rate in this region (larger than 500,000 s^{-1}). The viscosity in the collision region is approx. 10 mPa·s and shown in dark blue. Around the collision region, the liquid indicated in green is also significantly shear thinned and the viscosity is about 35 mPa·s, which is scarcely half as large as the zero viscosity of paint A. The viscosity of the liquid that is far away from the impact center remains unchanged. After the formation of a crater, the shear rate in the collision region is reduced and the viscosity is between 15 – 20 mPa·s accordingly. The green region, in which the liquid is heavily shear thinned, spreads

out of the collision region and enlarges to the maximum when the crater reaches the maximal depth. Subsequently, in the receding phase the viscosity of the liquid under the crater floor is quickly increased. High shear rate remains only in the region under the crater rim. In the end phase of the impact, the viscosity in the liquid film is increased to 70 – 75 mPa·s, namely quasi the zero viscosity of the model paint A. Small air bubbles that are entrained in the impact process can still be observed in the liquid film. They are still not in a stationary situation, oscillating in the film. Therefore, the liquid around the bubbles shows lower viscosity because of the shear thinning effect.

Effects of the shear thinning behaviour

For understanding the effect of the shear-thinning behaviour of paints on the droplet impact a comparative simulation with a Newtonian liquid was carried out. The Newtonian liquid used in the simulation has a viscosity of 80 mPa·s, namely corresponding to the zero viscosity of the model paint A. The surface tension of this liquid is also identical with that of the model paint A. The comparison of phenomena of the droplet impact with both liquids is shown in Figure 6. Here, the droplet diameter is 65 µm, the film thickness also 65 µm and the impact velocity 6 m/s. Both collisions result in the cratering impact. After falling onto the liquid film, the non-Newtonian drop connects the target liquid surface with a smooth shoulder, while a ruptured interface between the drop and the target liquid, a so-called drop neck, is observed in the Newtonian case. As the droplet falls into the film, a crater with smooth walls and a flat floor is quickly formed in the non-Newtonian liquid. In contrast, the crater wall in the Newtonian liquid is still ruptured and a banana-shaped construction can be found. Finally, a smooth crater can also be formed in the Newtonian liquid. Its size, both width and depth, is significantly greater than the crater of the non-Newtonian liquid.

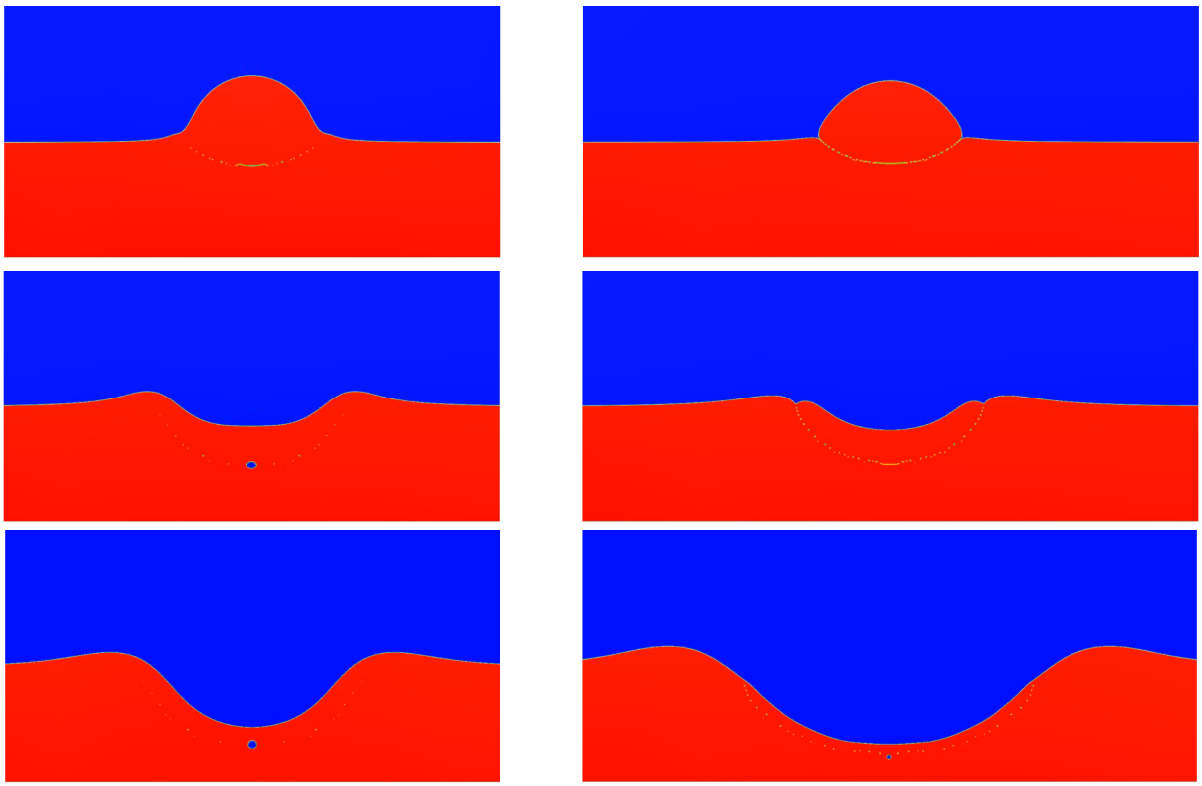

Figure 6. Phenomena of drop impacts on a wet solid surface (left: non-Newtonian model paint A, Re^{*}=24.16, We=89.75, Oh^{*}=0.39; right: Newtonian liquid, Re=4.48, We=89.75, Oh=2.11).

Crater size

The diameter of craters formed after the droplets impact into liquid films with various thickness could be determined in the simulation. The dimensionless crater sizes, namely the ratio between the crater diameter D_c and the droplet diameter d, are plotted as a function of the Reynolds number in Figure 7 a). In general, the crater size increases with an increasing Reynolds number. Under the same impact conditions, the craters of impacts on a thick film tend to be larger than the ones on a thin film. With increasing Reynolds number this difference becomes more and more evident and can be clearly observed if the Reynolds number is greater than 15. Taking into account the effect of the film thickness on the crater size, a characteristic non-dimensional diameter of the crater can be defined as follows:

$$D^* = \left(\frac{D_c}{d}\right)^{\frac{1}{Re^*}\cdot\left(\frac{h}{d}\right)^{-n}}$$

where Re^* is the characteristic Reynolds number of the drop and h the film thickness. The exponent *n* indicates the effect of the dimensionless film thickness on the crater size with $n = 0.1$. The characteristic crater size is plotted as a function of the Reynolds number in Figure 7 b). A strong correlation between both dimensionless values is observed.

$$D^* = A_0 + A_1 e^{-B\cdot Re}$$

where $A_0 = 1.07553$, $A_1 = 0.62629$ and $B = 0.19858$.

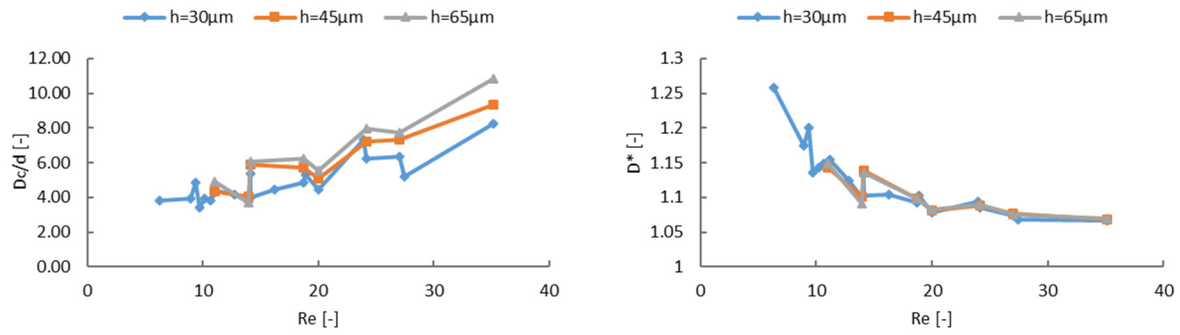

Figure 7. Crater sizes as a function of the Reynolds number.

Conclusions

As presented in this paper, numerical simulations based on the VOF model were carried out to study the impact of model paint droplets on solid surfaces covered by a thin paint film of identical fluid. The Cross model was used to describe the shear thinning behaviour of the model paints. The influence of this non-Newtonian behaviour on the droplet impact was discussed in comparison to the simulation with a Newtonian liquid. By varying the impact conditions, different phenomena of the impact could be observed, namely deposition and cratering. A boundary between both phenomena was found through a parameter study that reflects relevant conditions of spray painting processes with different atomizers. In general, a crater can be formed by the impact of a droplet whose Reynolds number is greater than 10. By contract, a depositing impact occurs at a lower Reynolds number if the Ohnesorge number of the droplet is also small. The width of the crater formed after the impact increases with

increasing Reynolds number. The characteristic crater diameter, in which also the effect of the film thickness is considered, was defined, indicating a strong correlation with the Reynold number. The simulation results deliver useful information for further investigations, such as flake orientation during droplet impact on wet solid surfaces, entrainment of air bubbles in the impact process as well as film leveling.

In future studies also 3D simulations will be carried out for selected cases based on the results of the 2D simulations shown in the present paper. The work will mainly focus on the entrainment of air bubbles in the impact process, which may lead to paint defects, such as pinholes, that result in a remaining reduction of the final paint film quality.

Acknowledgments
The present investigations were supported by the German Federal Ministry for Economical Affairs and Energy through the Arbeitsgemeinschaft industrieller Forschungsvereinigungen (AIF). The work was also supported by the High-Performance Computing Center (HLRS) of the University of Stuttgart.

References

[1] Worthington A. M., 1908, "A study of splashes."
[2] Šikalo, Š., Wilhelm, H.-D., Roisman, I. V., Jakirlić, S., and Tropea, C., 2005, Physics of Fluids, 17(6), p. 062103.
[3] Rein, M., 1993, "Phenomena of liquid drop impact on solid and liquid surfaces."
[4] Guo, Y., Lian, Y., and Sussman, M., 2016, Phys. Fluids, 28(7), p. 73303.
[5] Eggers, J., Fontelos, M. A., Josserand, C., and Zaleski, S., 2010, Physics of Fluids, 22(6), p. 62101.
[6] Blanchette, F., and Bigioni, T. P., 2009, J. Fluid Mech., 620, pp. 333–352.
[7] Lee, J. S., Park, S. J., Lee, J. H., Weon, B. M., Fezzaa, K., and Je, J. H., 2015, Nature communications, 6, p. 8187.
[8] Ye, Q., and Domnick, J., 2017, Journal of coatings technology research, 14(2), pp. 467–476.